



## Impedance Biosensor Incorporating a Carboxylate-Terminated Bidentate Thiol for Antibody Immobilization

Rajeswaran Radhakrishnan,<sup>a</sup> Madhavi Pali,<sup>b,\*</sup> Han Ju Lee,<sup>c</sup> T. Randall Lee,<sup>c</sup> and Ian I. Suni<sup>b,\*\*,z</sup>

<sup>a</sup>Materials Science and Engineering, Clarkson University, Potsdam, New York 13699, USA

<sup>b</sup>Materials Technology Center, Department of Mechanical Engineering and Energy Processes, Department of Chemistry and Biochemistry, Southern Illinois University, Carbondale, Illinois 62901, USA

<sup>c</sup>Department of Chemistry and the Texas Center for Superconductivity, University of Houston, Houston, Texas 77204-5003, USA

An impedance biosensor is reported that employs the bidentate thiol, 16-[3,5-bis(mercaptopethyl)phenoxy]-hexadecanoic acid (BMPHA), as a bifunctional reagent for antibody immobilization atop an Au electrode, and the results are compared to those obtained for the analogous monodentate reagent, 16-mercaptophexadecanoic acid (16 MHA). The detection limit for peanut protein Ara h 1 on the BMPHA bidentate thiol-coated Au electrode is approximately 0.71 ng/mL (0.01 nM), about 3x lower than that obtained on the comparable monodentate (16-MHA) thiol-coated Au electrode. Daily impedance measurements were employed to study antibody regeneration with a mild denaturing agent, 0.2 M KSCN at pH 7.3. The antibody-coated electrodes retained activity toward Ara h1 for 10 and 20 days of regeneration of the monodentate- and BMPHA-coated Au electrodes, respectively, illustrating the superior stability of protein films atop the BMPHA bidentate thiol.

© 2016 The Electrochemical Society. [DOI: [10.1149/2.0301605jes](https://doi.org/10.1149/2.0301605jes)] All rights reserved.

Manuscript submitted September 1, 2015; revised manuscript received December 23, 2015. Published January 20, 2016.

Biomolecule immobilization onto metallic surfaces through self-assembled monolayers (SAMs) is attractive for biosensing because (1) the short length of the linker chain allows for electrical interrogation, and (2) covalent bond formation to proteins allows for the creation of a stable interface. SAMs are also ideal systems for fundamental and applied studies of electro-optic devices, corrosion, lubrication, adhesion, biocatalysis, molecular recognition, and sensing devices.<sup>1</sup> Many combinations of metal surfaces and organic molecules have been studied for SAM formation, but alkane thiol SAMs on noble metal surfaces (especially Au) have attracted the most interest for preparing structurally well-defined chemical interfaces, and thin films with controllable thickness and desired functions.<sup>2</sup>

Au-thiol self-assembled monolayers (SAM) are often employed for protein immobilization within electrochemical biosensors, since Au is both electrically conductive and biocompatible. Electrochemical impedance spectroscopy has been widely studied for biosensor applications as a method for transduction of biomolecular recognition.<sup>3-5</sup> Impedance biosensors are simpler than most other methods, since they have no optical or acoustic components, making them ideal for portable and implantable applications.<sup>6</sup> Although impedance biosensors have been widely studied, applications have been limited by possible insensitivity to small analytes, susceptibility to nonspecific adsorption, and stability of biomolecule immobilization, which typically employs Au-thiol chemistry.<sup>7</sup>

For such applications, the utility of Au-alkanethiol SAMs has been limited by instability upon exposure to high temperature,<sup>8,9</sup> ultraviolet light,<sup>10,11</sup> and/or harsh chemical reagents.<sup>12,13</sup> A significant increase in stability has been reported for multidentate relative to monodentate thiol adsorbates,<sup>14-16</sup> in part because the free energy of the entropically favored bidentate binding can be twice that of monodentate binding.<sup>17,18</sup> One of our research groups recently reported SAM formation on Au from the bidentate thiol 16-[3,5-bis(mercaptopethyl)phenoxy]-hexadecanoic acid (BMPHA).<sup>19</sup> The other group recently reported impedance biosensing of peanut protein Ara h 1, an allergenic food protein.<sup>20,21</sup> Biosensors for detection of peanut proteins, and other food allergens, has recently attracted significant interest. Peanuts are a particularly problematic food allergen due to the prevalence of peanuts in a wide variety of food products, the high sensitivity of some individuals, and the stability of some allergenic peanut proteins during food manufacturing and human digestion.<sup>22-25</sup> Here, incorporation of BMPHA as a linker reagent is reported for

an impedance biosensor to detect peanut protein Ara h 1, as well as studies of antibody regeneration in 0.2 M KSCN for up to 20 days.

### Experimental

**Materials.**—Glass slides with a 100-nm Au film atop a 5-nm Ti adhesion layer were purchased from Evaporated Metal Films (Ithaca, NY); 16-mercaptophexadecanoic acid (16-MHA) was purchased from Santa Cruz biotechnology; N-(3-dimethylaminopropyl)-N'-(ethylcarbodiimide hydrochloride) (EDC), potassium dihydrogen phosphate, and di-potassium dihydrogen phosphate were purchased from Sigma; N-hydroxysulfosuccinimide sodium salt (NHSS) was purchased from Pierce biotechnology; ethanol, potassium thiocyanate, and tetrahydrofuran were purchased from Fisher Scientific; and potassium ferri/ferrocyanide was purchased from Acros Organics. Peanut protein Ara h 1 and its mouse monoclonal IgG<sub>1</sub> antibody were purchased from Indoor Biotechnologies. Polyclonal cortisol antibody was purchased from Sigma Aldrich, and *Cyprinus carpio* vitellogenin and its mouse monoclonal IgG<sub>1</sub> antibody were purchased from Cayman Chemical. 16-[3,5-bis(mercaptopethyl)phenoxy]-hexadecanoic acid (BMPHA) was synthesized at the University of Houston according to published protocols.<sup>19</sup>

**Au electrode and biosensor preparation.**—Sensor preparation and antibody immobilization followed previously published protocols. The Au electrode was fixed by an O-ring onto an electrochemical cell constructed from virgin Teflon. The conical electrochemical cell was designed with an electrode area of 0.19 cm<sup>2</sup> and a cell volume of 6 mL. The monodentate thiol monolayer with 16-MHA and bidentate thiol monolayer with BMPHA were formed by immersing an Au electrode into 3 mM ethanoic solutions of 16-MHA and BMPHA for 48 hours at 4–6°C. After 48 hours, the electrodes were cleaned with distilled water, ethanol, and tetrahydrofuran, followed by drying in Ar. For both monodentate and bidentate thiol films, the terminal carboxylate groups were activated for 1 hour in 75 mM EDC and 15 mM NHSS in 50 mM phosphate buffer solution (pH = 7.3). The antibody-coated electrodes are then created by immersion for 1 hour into a solution containing 50 µg/mL antibody and 50 mM PBS at pH 7.3, forming amide bonds to amine groups on the protein surface. Non-specific adsorption was reduced by immersing the antibody-coated electrodes in 0.1% BSA for 1 hour. These sensor electrodes were then exposed to increasing concentrations of peanut protein Ara h 1.

For the antibody regeneration experiments, the Au electrodes were exposed to 0.2 M KSCN at pH 7.3 to release the analyte from antibody, followed by storage in 0.1 M BSA and 50 mM PBS buffer. The

\*Electrochemical Society Student Member.

\*\*Electrochemical Society Member.

<sup>z</sup>E-mail: [isuni@siu.edu](mailto:isuni@siu.edu)

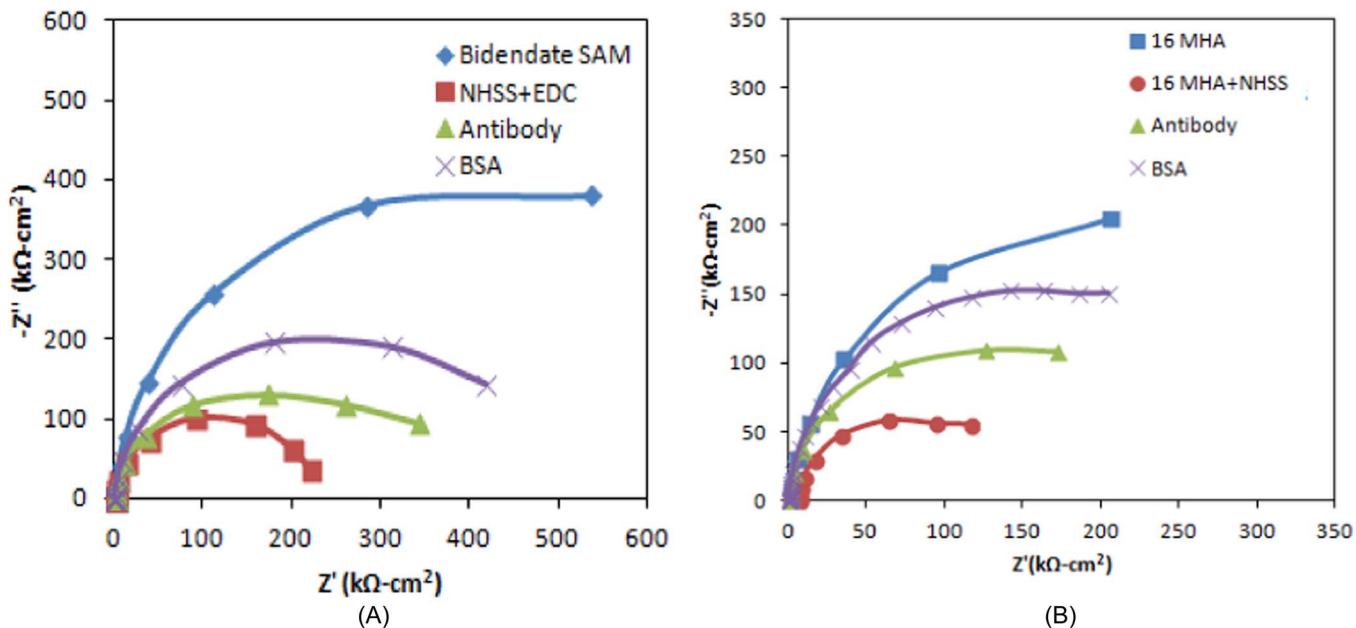


**Figure 1.** Nyquist plots of the impedance response during interface fabrication using the BMPHA (A) and 16-MHA (B) adsorbates.

electrodes were then exposed to increasing concentrations of peanut protein Ara h 1. This procedure was repeated twice each day until the antibody was observed to lose its activity toward antigen binding.

**Electrochemical measurements.**—All electrochemical measurements were performed with a three-electrode configuration using a Pt spiral counter electrode and an Ag/AgCl reference electrode. The background test solution contained 50 mM PBS and 5 mM  $\text{K}_3\text{Fe}(\text{CN})_6/\text{K}_4\text{Fe}(\text{CN})_6$  at pH 7.3, with varying concentrations of the target analyte. Impedance measurements were performed using a Gamry Instruments Reference 600 over the frequency range from 0.05 Hz to 15 kHz with an AC probe amplitude of 5 mV. Each impedance spectrum takes about 2.8 min to acquire. The impedance results were obtained at a DC potential of +200 mV vs. Ag/AgCl, which is close to the open circuit potential (OCP) of the  $\text{Fe}(\text{CN})_6^{3-/-4-}$  redox probe.

**Other measurements.**—Quartz crystal microbalance measurements were performed at open circuit using a CHI 410C (CH Instruments, Austin TX) coupled with an Au-coated quartz oscillator over the period of 14 hours in 50 mM PBS buffer at pH 7.3. Spectroscopic ellipsometry measurements were performed *in situ* on the polymer-protein films using a J. A. Woollam M44 spectroscopic ellipsometer at wavelengths of 420–760 nm at a fixed angle of incidence of 70° from the surface normal in 50 mM PBS buffer at pH 7.3. The effective refractive index of the original Au film was determined by ellipsometry measurements, and used for all subsequent polymer-protein film studies. A refractive index of 1.45 was assumed for all polymer-protein film measurements. The reproducibility of ellipsometric determination of film thickness was within  $\pm 0.2$  nm.

## Results and Discussion

**Impedance studies of electrode preparation, antigen binding, sensitivity and selectivity.**—Figures 1A and 1B illustrate Nyquist plots of the impedance spectra after self-assembled monolayer (SAM) formation from BMPHA and 16-MHA, activation with EDC + NHSS, and immobilization of the antibody to Ara h 1, followed by immersion of 0.1% BSA. The supporting electrolytes are 50 mM PBS buffer and 5 mM  $\text{K}_3\text{Fe}(\text{CN})_6/\text{K}_4\text{Fe}(\text{CN})_6$  at pH 7.3. The impedance spectra in Figures 1A and 1B can be fit with a Randles equivalent circuit with the differential capacitance ( $C_d$ ) replaced with a constant phase

element (CPE), as shown in Figure 2. Here,  $R_s$  corresponds to the solution phase resistance, and  $R_{ct}$  to the charge transfer resistance. The Randles equivalent circuit, with or without a CPE, has been widely employed to model biosensor interfaces,<sup>26,27</sup> since electrochemical reactions such as corrosion that result in more complex impedance signatures are blocked by the adsorbed polymer-protein film. The impedance of the CPE is:<sup>28–30</sup>

$$Z(CPE) = \frac{1}{T(j\omega)^n} \quad [1]$$

where  $T$  is a frequency-independent constant,  $\omega$  is the angular frequency, and  $n$  is an exponent within the range  $0.5 < n < 1$ . The results in Figures 1A and 1B were analyzed by complex non-linear least squares (CNLS) regression, and the best-fit equivalent circuit parameters and standard errors are given in Tables IA and IB, respectively. In all cases, the exponent  $n$  is close to unity, validating use of a CPE. The unusually large values for  $R_{ct}$  following SAM formation from BMPHA and 16-MHA arise due to electrostatic repulsion between the exposed carboxylate groups and the redox probe,  $\text{Fe}(\text{CN})_6^{4-/-3-}$ . If the positively charged redox probe  $\text{Ru}(\text{NH}_3)_6^{3+/4+}$  is substituted for  $\text{Fe}(\text{CN})_6^{4-/-3-}$ , then  $R_{ct}$  values at negatively charged interfaces are reduced by approximately 3–10x.<sup>31–33</sup>

Figures 3A and 3B illustrate Nyquist plots for the impedance response to increasing concentrations of peanut protein Ara h 1. The results were fit to the same equivalent circuit, and the best-fit parameters and standard errors are given in Tables II A and II B. The charge transfer resistance ( $R_{ct}$ ), which is approximately the diameter of the semicircular plots in Figures 3A and 3B, is the most sensitive circuit element in Tables II A and II B to binding of peanut protein Ara h 1.  $R_{ct}$  initially increases with increasing concentration of Ara h 1, and eventually approaches a maximum value due to saturation of the antibody film, as shown in Figures 4A and 4B. Such behavior is commonly

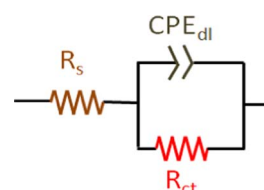


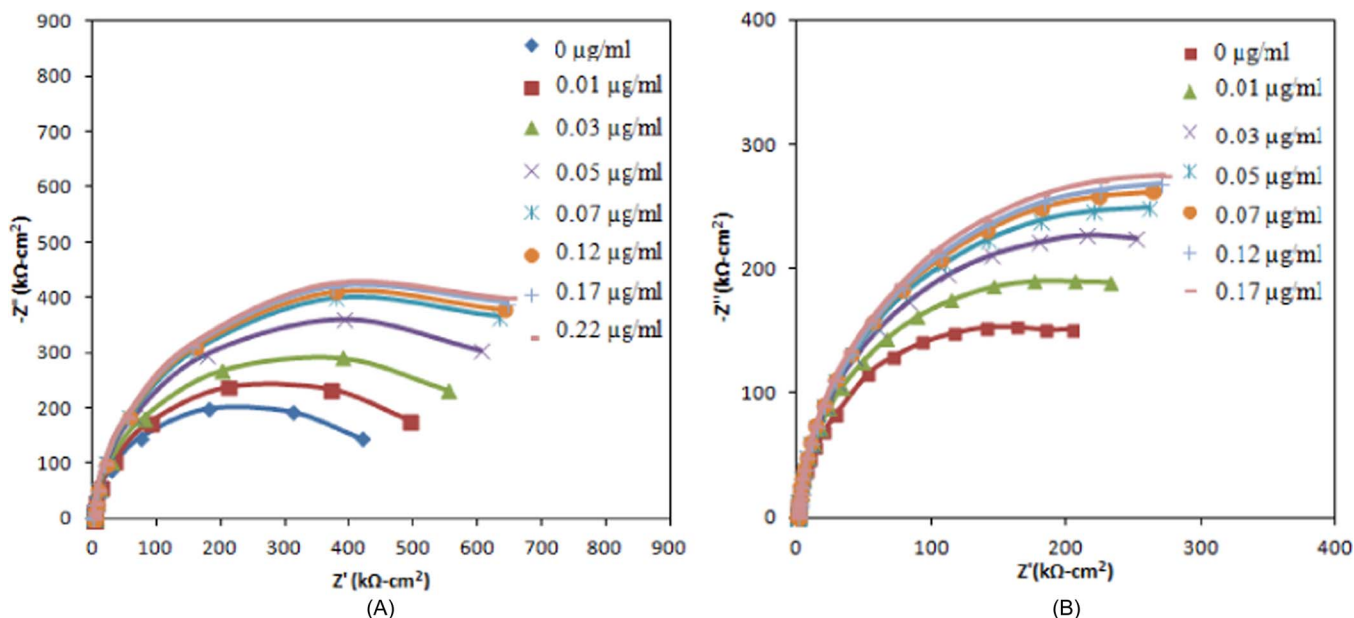
**Figure 2.** Randles equivalent circuit.

**Table I.** Best-fit equivalent circuit parameters (standard error) during fabrication of antibody-coated electrode using BMPHA (A) and 16-MHA (B).

Circuit Parameters	Bidentate SAM	NHSS+EDC	Antibody	BSA
$R_s$ ( $\Omega \cdot \text{cm}^2$ )	45.8 (0.2)	42.2 (0.2)	45.1 (0.3)	44.62 (0.3)
$CPE-T$ ( $\mu\text{F cm}^{-2} \text{s}^{n-1}$ )	2.25 (0.01)	2.31 (0.01)	2.37 (0.02)	2.41 (0.01)
$n$	0.95 (0.001)	0.95 (0.002)	0.94 (0.001)	0.95 (0.001)
$R_{ct}$ ( $\text{k}\Omega \cdot \text{cm}^2$ )	1066 (10.2)	226 (1.3)	331 (7.4)	457 (6.7)
(A)				
$R_s$ ( $\Omega \cdot \text{cm}^2$ )	15.8 (0.2)	19.2 (0.2)	20.1 (0.3)	24.62 (0.3)
$CPE-T$ ( $\mu\text{F cm}^{-2} \text{s}^{n-1}$ )	2.13 (0.01)	2.22 (0.01)	2.30 (0.02)	2.48 (0.01)
$n$	0.96 (0.001)	0.95 (0.002)	0.95 (0.001)	0.96 (0.001)
$R_{ct}$ ( $\text{k}\Omega \cdot \text{cm}^2$ )	438 (3.2)	186 (1.3)	298 (7.4)	320 (4.5)
(B)				

observed for the Langmuir adsorption isotherm and arises from competition for binding sites when antibody-antigen binding is much stronger than interactions between adjacent antibody molecules.<sup>20,21</sup> Antigen binding was also studied atop the antibody-coated sensor electrode constructed from the BMPHA bidentate thiol by quartz crystal microbalance (Supplementary Information, Figure S1 and Table S1) and spectroscopic ellipsometry (Supplementary Informa-

tion, Table S2). In both cases, the results are also consistent with the Langmuir adsorption isotherm, where the polymer-protein film thickness initially increases linearly with Ara h 1 concentration, and eventually saturates at high concentration. The quartz crystal microbalance and spectroscopic ellipsometry results demonstrate that the antibody surface coverage atop BMPHA and 16-MHA are quite similar.

**Figure 3.** Nyquist plots of the impedance response to increasing concentrations of peanut protein Ara h 1 at the interface fabricated with BMPHA (A) and 16-MHA (B).**Table II.** Best-fit equivalent circuit parameters (standard error) during exposure of antibody-coated electrode with BMPHA (A) and 16-MHA (B) to increasing concentrations of peanut protein Ara h 1.

Concentration of Ara h 1 ( $\mu\text{g/mL}$ )	0	0.01	0.03	0.05	0.07	0.12	0.17	0.22
$R_s$ ( $\Omega \cdot \text{cm}^2$ )	44.62(0.3)	45.42(0.4)	43.77(0.4)	44.80(0.3)	44.41(0.3)	43.82(0.4)	43.25(0.4)	42.78 (0.3)
$CPE-T$ ( $\mu\text{F cm}^{-2} \text{s}^{n-1}$ )	2.41 (0.01)	1.99 (0.01)	2.03 (0.01)	2.10 (0.01)	2.18 (0.01)	2.18 (0.01)	2.19 (0.01)	2.20 (0.01)
$n$	0.95 (0.001)	0.95 (0.001)	0.95 (0.001)	0.95 (0.001)	0.95 (0.001)	0.95 (0.001)	0.95 (0.001)	0.95 (0.001)
$R_{ct}$ ( $\text{k}\Omega \cdot \text{cm}^2$ )	457.8 (6.7)	545.1 (6.6)	645.6 (6.9)	777.9 (6.8)	870.1 (6.9)	899.9 (6.9)	922.8 (6.1)	938.4 (6.4)
(A)								
$R_s$ ( $\Omega \cdot \text{cm}^2$ )	24.62 (0.3)	25.42 (0.4)	23.77 (0.4)	24.80 (0.3)	24.41 (0.3)	23.82 (0.4)	23.25 (0.4)	22.78 (0.3)
$CPE-T$ ( $\mu\text{F cm}^{-2} \text{s}^{n-1}$ )	2.48 (0.01)	2.29 (0.01)	2.09 (0.01)	1.90 (0.01)	1.85 (0.01)	1.82 (0.01)	1.82 (0.01)	1.80 (0.01)
$n$	0.96 (0.001)	0.95 (0.001)	0.94 (0.001)	0.94 (0.001)	0.95 (0.001)	0.95 (0.001)	0.96 (0.001)	0.95 (0.001)
$R_{ct}$ ( $\text{k}\Omega \cdot \text{cm}^2$ )	320.1 (4.5)	439.2 (5.9)	525.8 (6.2)	617.9 (6.7)	701.1 (5.9)	772.1 (6.4)	802.8 (6.5)	838.4 (6.4)
(B)								

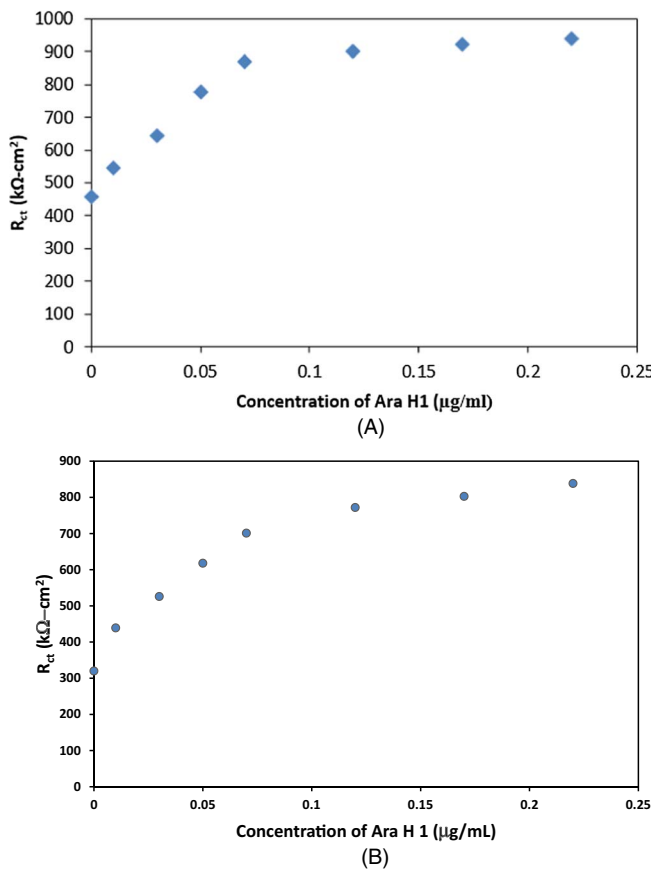
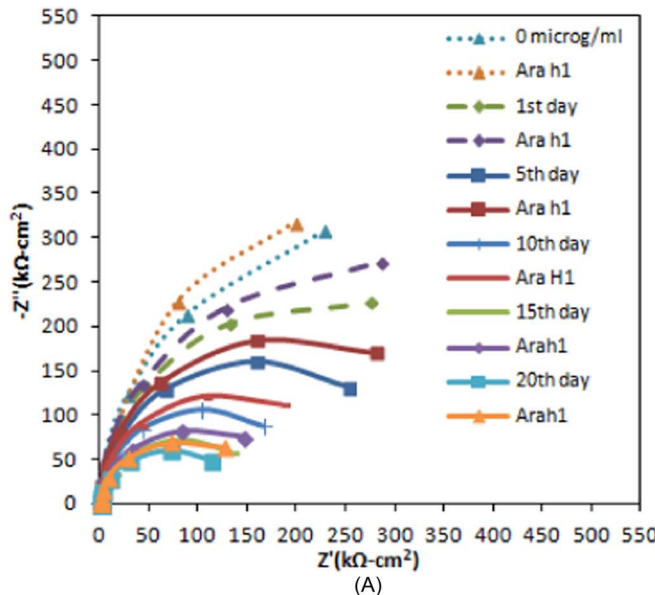


**Figure 4.** Variation in the charge transfer resistance ( $R_{ct}$ ) with concentration of peanut protein Ara h 1 for antibody film atop BMPHA (A) and 16-MHA (B).

The detection limit for impedance biosensing of peanut protein Ara h 1 can be determined from:

$$\text{Detection Limit} = \frac{3\sigma}{\text{Sensitivity}} \quad [2]$$



where the standard deviation is determined from repeated measurements of  $R_{ct}$  on electrolytes containing no antigen, and the sensitivity is the initial slope of Figures 4A and 4B. This yields sensitivities of  $6.6 (\text{M}\Omega\cdot\text{cm}^2)/(\mu\text{g}/\text{mL})$  and  $4.6 (\text{M}\Omega\cdot\text{cm}^2)/(\mu\text{g}/\text{mL})$  for the antibody film atop the bidentate thiol BMPHA and antibody film atop the monodentate thiol, 16-MHA. This approach yields a detection limit for Ara h 1 of approximately  $0.71 \text{ ng}/\text{mL}$  ( $0.01 \text{ nM}$ ) for the antibody film atop the bidentate thiol BMPHA, about 3x lower than the detection limit of  $2.1 \text{ ng}/\text{mL}$  ( $0.03 \text{ nM}$ ) obtained atop the monodentate thiol, 16-MHA. Given that the density of carboxylate groups on the BMPHA SAM is  $\sim 45\%$  that of the 16-MHA SAM,<sup>19</sup> antibodies on the BMPHA SAM might be immobilized through fewer amide bonds, making them more loosely packed and sterically unencumbered than those on the 16-MHA SAM. Steric freedom has been shown to enhance antibody activity at interfaces.<sup>34,35</sup>

Selectivity was also investigated by exposing sensor electrodes created atop by BMPHA and 16-MHA to high concentrations ( $16 \mu\text{g}/\text{mL}$ ) of *Cyprinus carpio* vitellogenin, the mouse monoclonal antibody to this vitellogenin, and the polyclonal antibody to cortisol. In all three cases, the impedance response to introduction of these proteins was unmeasurable, indicating that the selectivity with respect for peanut protein Ara h 1 is close to unity. The high selectivity obtained here is analogous to previously reported results for impedance detection of *Listeria monocytogenes*, which was highly selective with respect to *Salmonella enterica*.<sup>36</sup> Such results demonstrate that the use of BSA for site blocking is effective for minimizing non-specific adsorption.

**Long-term studies of antibody film regeneration.**—Biosensors must typically be calibrated due to variations between sensors created on different days, or under slightly different conditions. For example, test strips for handheld glucose biosensors might be calibrated in both blood plasma and/or whole blood, while transdermal glucose biosensors may be calibrated *in vivo*.<sup>37</sup> For antibody-based impedance biosensors, this requires repeated unfolding of the antibody film to release the bound antigen. Antibody-based ELISA tests typically allow 50–60 cycles of regeneration, most commonly using strong acids or bases as chaotropic reagents.<sup>38</sup> However, for the current biosensor interface, where a protein film is immobilized atop an Au-thiol self-assembled monolayer (SAM), strong chaotropic reagents such as NaOH and glycine-HCl cause the antibody film to lose its activity toward peanut protein Ara h 1 after only one regeneration cycle (results not shown). Therefore, a gentler chaotropic reagent ( $0.2 \text{ M}$  KSCN at

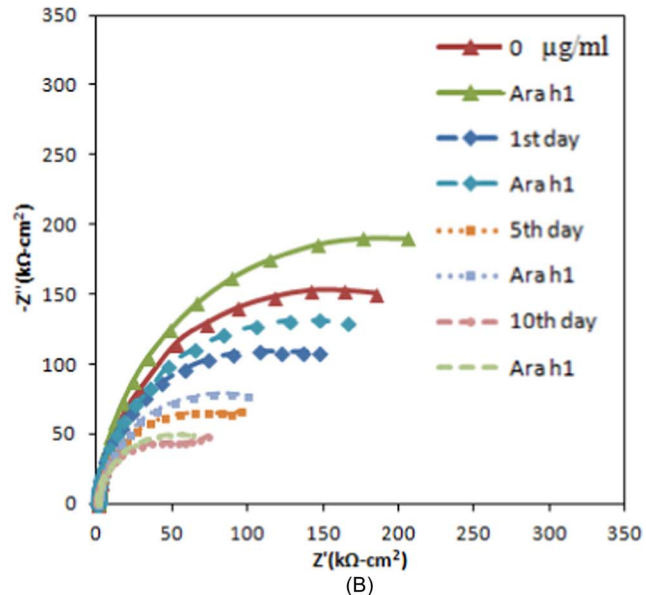


**Figure 5.** Impedance spectra of antibody film atop SAM created from BMPHA (A) and 16-MHA (B) before and after exposure to  $0.05 \mu\text{g}/\text{mL}$  peanut protein Ara h 1, following daily antibody regeneration with  $0.2 \text{ M}$  KSCN.

**Table III.** Best-fit equivalent circuit parameters (standard errors) during daily antibody regeneration for electrodes fabricated from monodentate and bidentate thiols.

16-MHA-coated electrode $R_{ct}$ ( $\text{k}\Omega\cdot\text{cm}^2$ )		
Days	Bare antibody	0.05 $\mu\text{g/mL}$ Ara h1
0	320 (4.5)	617 (6.7)
1	270 (6.7)	347 (7.1)
5	159 (6.5)	183 (7.1)
10	94 (6.2)	117 (6.9)
BMPHA-coated electrode $R_{ct}$ ( $\text{k}\Omega\cdot\text{cm}^2$ )		
Days	Bare antibody	0.05 $\mu\text{g/mL}$ Ara h1
0	630 (7.6)	677 (7.1)
1	538 (7.7)	581 (7.1)
5	379 (7.2)	453 (7.5)
10	254 (7.5)	332 (7.3)
15	196 (7.4)	228 (7.1)
20	162 (7.5)	180 (7.3)

pH 7.3)<sup>39</sup> was utilized for regeneration of the impedance biosensor for peanut protein Ara h 1, using antibody films immobilized atop both bidentate thiol BMPHA and monodentate thiol 16-MHA.

The antibody-coated Au electrodes were stored in 50 mM PBS buffer at pH 7.3 between regeneration studies and interrogated daily by the following sequence:

- 1) Exposure to increasing concentrations (0.01, 0.03, 0.05, 0.12 and 0.17  $\mu\text{g/mL}$ ) of peanut protein Ara h1.
- 2) Exposure to 0.2 M KSCN (pH 7.3) to unfold the antibody film.
- 3) Exposure to 0.1 M BSA and 50 mM PBS buffer to refold the antibody film.
- 4) Storage in 50 mM PBS buffer at pH 7.3.

The Nyquist plots illustrating regeneration of antibody-coated Au electrodes for bidentate thiol BMPHA and monodentate thiol 16-MHA are shown in Figure 5A and 5B, respectively.

To aid visualization, only the data taken every five days for the BMPHA electrode and 16-MHA electrode are shown. The best-fit Randles equivalent circuit parameters obtained during these experiments are given in Table III. The antibody-coated Au electrode retained its activity toward Ara h 1 for 10 and 20 days of regeneration of the 16-MHA- and BMPHA-coated Au electrodes, respectively. This comparison illustrates the superior stability of protein films atop the bidentate BMPHA-coated Au electrode relative to the monodentate 16-MHA-coated Au electrode. Further, these studies illustrate that protein immobilization through Au-thiol self-assembled monolayers (SAMs) has better storage stability than might be expected. For example, rapid degradation on a time scale of hours to tens of hours has been reported for SAMs stored in air<sup>40-43</sup> and in cell culture media.<sup>44</sup> On the other hand, stability on a length scale of days to weeks has been reported for SAMs stored in aqueous solutions.<sup>45,46</sup> The stability observed here, with a protein covalently immobilized onto a carboxylate-terminated SAM, is therefore similar to that reported for bare SAMs stored in aqueous solution.

The accurate calibration of the BMPHA-coated impedance biosensor during consecutive experiments on the third day is illustrated by the Nyquist plots in Figure 6 using the procedures described above. Here the closed symbols correspond to the first exposure to increasing Ara h 1 concentration, and the open symbols correspond to a second exposure to increasing Ara h 1 concentration, following antibody unfolding and refolding. As shown in Figure 6, the detection accuracy within one day is typically ~2%. This illustrates that these impedance biosensors can be stored for an extended period of time, and although the interface degrades to some extent, they can be accurately calibrated when needed for Ara h 1 detection.

Impedance detection of peanut protein Ara h 1, and other allergenic food proteins, may allow rapid and inexpensive detection of food

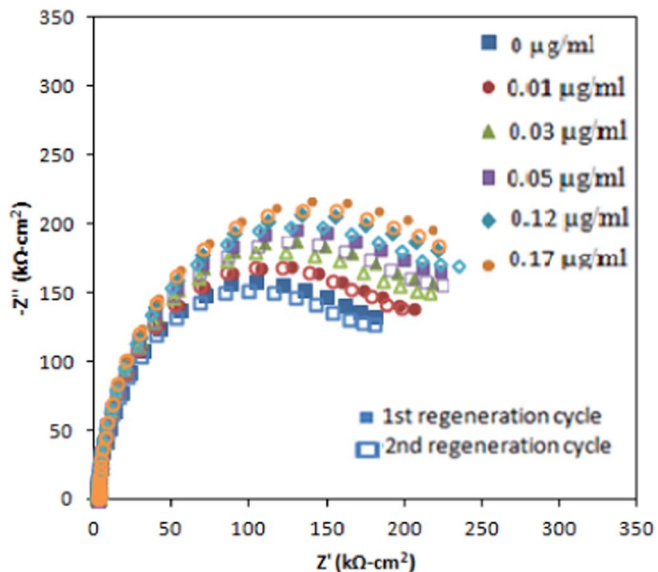


**Figure 6.** Nyquist plots of impedance spectra during two consecutive trials for peanut antibody regeneration with 0.2 M KSCN on BMPHA-coated electrode within one day (Third day of experiment).

allergens by either consumers or food service companies. Food allergens are most commonly detected by immunoassays such as ELISA, DNA-based methods such as polymerase chain reaction (PCR), and mass spectrometry.<sup>23</sup> Unfortunately, these methods are slow, difficult to automate, and difficult to multiplex. Recently biosensors based on a variety of different methods, including electrochemical impedance spectroscopy (EIS), have been investigated for rapid, inexpensive and multiplexed detection of food allergens.<sup>24</sup> The technical challenges for applications of impedance biosensors have been recently reviewed,<sup>7</sup> and include the stability and reproducibility of biomolecular immobilization at a conductive electrode surface, non-specific adsorption in complex media, and the increased difficulty of AC impedance detection relative to DC electrochemistry. The current report focuses on the first challenge, improving the stability of biomolecular immobilization at Au electrodes, which are the most commonly employed substrates.

## Conclusions

The mouse monoclonal antibody to peanut protein Ara h 1 was immobilized onto two different Au sensor electrodes, one that employs the bidentate thiol, 16-[3,5-bis(mercaptopethyl)phenoxy]-hexadecanoic acid (BMPHA), as a bifunctional reagent, and one that employs the comparable monodentate reagent, 16-mercaptophexadecanoic acid (16-MHA). These sensor electrodes were tested for impedance biosensing of Ara h 1, and the detection limit on the BMPHA bidentate thiol-coated Au electrode is approximately 0.71 ng/mL (0.01 nM), about 3x lower than that obtained using 16-MHA. Antigen binding was also studied quantitatively using a quartz crystal microbalance and spectroscopic ellipsometry, yielding a dependence on Ara h 1 concentration closely similar to that observed during impedance measurements. For all three methods, the response as a function of Ara h 1 appeared to follow the Langmuir adsorption isotherm, with a linear response at low antigen concentration, but eventual saturation at high antigen concentrations as the antibody binding sites become filled. Antibody regeneration was studied daily using a mild denaturing agent, 0.2 M KSCN at pH 7.3. The antibody-coated on Au electrodes retained activity toward Ara h 1 for 10 and 20 days of regeneration of the monodentate- and BMPHA-coated Au electrodes, respectively, illustrating the superior stability of protein films atop the BMPHA bidentate thiol.

### Acknowledgments

This research was supported by NSF grant # ECCS-1342618. Additional support for the research at the University of Houston was provided by the Robert A. Welch Foundation (grant No. E-1320), the National Science Foundation (DMR-0906727 and CHE-1411265), and the Texas Center for Superconductivity at the University of Houston.

### References

1. H. G. Hong and W. Park, *Langmuir*, **17**, 2485 (2001).
2. J. C. Love, L. A. Estroff, J. K. Kriebel, R. G. Nuzzo, and G. M. Whitesides, *Chem. Rev.*, **105**, 1103 (2005).
3. E. Katz and I. Willner, *Electroanal.*, **15**, 913 (2009).
4. L. Yang and R. Bashir, *Biotechnol. Adv.*, **26**(2), 135 (2008).
5. M. I. Prodromidis, *Electrochim. Acta*, **55**, 4227 (2010).
6. S. Laschi and M. Mascini, *Med. Eng. Phys.*, **28**, 934 (2006).
7. R. Radhakrishnan, I. I. Suni, C. S. Bever, and B. D. Hammock, *ACS Sustain. Chem. Engin.*, **2**, 1649 (2014).
8. C. D. Bain, E. B. Troughton, Y. T. Tao, J. Evall, G. M. Whitesides, and R. G. Nuzzo, *J. Am. Chem. Soc.*, **111**, 321 (1989).
9. F. Bensebaa, T. H. Ellis, A. Badia, and R. B. Lennox, *J. Vac. Sci. Technol. A*, **13**, 1331 (1995).
10. J. Huang and J. C. Hemminger, *J. Am. Chem. Soc.*, **115**, 3342 (1993).
11. S. W. Tam-Chang, H. A. Biebuyck, G. M. Whitesides, N. Jeon, and R. G. Nuzzo, *Langmuir*, **11**, 4371 (1995).
12. F. P. Zamborini and R. M. Crooks, *Langmuir*, **13**, 122 (1997).
13. R. G. Nuzzo, F. A. Fusco, and D. L. Allara, *J. Am. Chem. Soc.*, **109**, 2358 (1987).
14. L. Srisombat, S. Zhang, and T. R. Lee, *Langmuir*, **26**, 41 (2010).
15. S. Perumal, A. Hofmann, N. Scholz, E. Rühl, and C. Graf, *Langmuir*, **27**, 4456 (2011).
16. D. Ge, X. Wang, K. Williams, and R. Levicky, *Langmuir*, **28**, 8446 (2012).
17. P. Chinwangso, A. C. Jamison, and T. R. Lee, *Acc. Chem. Res.*, **44**, 511 (2011).
18. L. Srisombat, A. C. Jamison, and T. R. Lee, *Colloids Surf. A*, **390**, 1 (2011).
19. H. J. Lee, A. C. Jamison, Y. H. Yuan, C. H. Li, S. Rittikulsittichai, L. Rusakova, and T. R. Lee, *Langmuir*, **29**, 10432 (2013).
20. Y. Huang, M. Bell, and I. I. Suni, *Anal. Chem.*, **80**, 9157 (2008).
21. Y. Huang and I. I. Suni, *J. Electrochem. Soc.*, **155**, J350 (2008).
22. R. Pilolli, L. Monaci, and A. Visconti, *Trends Anal. Chem.*, **47**, 12 (2013).
23. M. Peeters, K. Jiménez-Monroy, C. Libert, Y. Eurlings, W. Cuypers, G. Wackers, S. Duchateau, P. Robaeys, M. Nesládek, B. van Grinsven, E. Pérez-Ruiz, J. Lamertyn, P. Losada-Pérez, and P. Wagner, *J. Biosens. Bioelectron.*, **5**, 1555 (2014).
24. R. C. Alves, F. B. Pimentel, H. P. A. Nouws, W. Correr, M. Begoña González-García, M. B. P. P. Oliveira, and C. Delerue-Matos, *Anal. Bioanal. Chem.*, **407**, 7157 (2015).
25. V. R. V. Montiel, S. Campuzano, A. Pellicanò, R. M. Torrente-Rodríguez, A. J. Reviejo, M. S. Cosío, and J. M. Pingarrón, *Anal. Chim. Acta*, **880**, 52 (2015).
26. I. I. Suni, *Trends Anal. Chem.*, **27**, 604 (2008).
27. Q. Xu and J. J. Davis, *Electroanal.*, **26**, 1249 (2014).
28. U. Rammelt and G. Reinhard, *Electrochim. Acta*, **35**, 1045 (1990).
29. T. Pajkossy, *J. Electroanal. Chem.*, **364**, 111 (1994).
30. K. Juttner, *Electrochim. Acta*, **35**, 1501 (1990).
31. N. Gua, D. Wei, L. Niu, and A. Ivaska, *Electrochim. Acta*, **51**, 6038 (2006).
32. W. Sanders, R. Vargas, and M. R. Anderson, *Langmuir*, **24**, 6133 (2008).
33. D. M. Fernandes, M. E. Ghica, A. M. V. Cavaleiro, and C. M. A. Brett, *Electrochim. Acta*, **56**, 7940 (2011).
34. R. Fishler, A. Artzy-Schnirman, E. Peer, R. Wolchinsky, R. Brener, T. Waks, Z. Eshhar, Y. Reiter, and U. Sivan, *Nano Lett.*, **12**, 4992 (2012).
35. A. Makaraviciute and A. Ramanaviciene, *Biosens. Bioelectron.*, **50**, 460 (2013).
36. R. Radhakrishnan, M. Jahne, S. W. Rogers, and I. I. Suni, *Electroanal.*, **25**, 2231 (2013).
37. A. Heller and B. Feldman, *Chem. Rev.*, **108**, 2482 (2008).
38. J. W. Chung, S. D. Kim, R. Bernhardt, and J. C. Pyun, *Sens. Actuat. B*, **114**, 1007 (2006), and references therein.
39. L. Locascio-Brown, A. L. Plant, V. Horvath, and R. A. Durst, *Anal. Chem.*, **62**, 2587 (1990).
40. M. H. Schoenfisch and J. E. Pemberton, *J. Am. Chem. Soc.*, **120**, 4502 (1998).
41. M. T. Lee, C. C. Hsueh, N. S. Freund, and G. S. Ferguson, *Langmuir*, **14**, 6419 (1998).
42. Y. Zhang, R. H. Terrill, and P. W. Bohn, *Chem. Mater.*, **11**, 2191 (1999).
43. T. M. Willey, A. L. Vance, T. Van Buuren, C. Bostedt, L. J. Terminello, and C. S. Fadley, *Surf. Sci.*, **576**, 188 (2005).
44. J. Maciel, M. C. L. Martins, and M. A. Barbosa, *J. Biomed. Mater. Res. A*, **94**, 833 (2010).
45. B. Y. Kong, Y. S. Kim, and I. S. Choi, *Bull. Korean Chem. Soc.*, **29**, 1843 (2008).
46. G. T. Qin and C. Z. Cai, *Chem. Commun.*, **2009**, 5112 (2009).